J Mater Sci (2008) 43:5076–5082
DOI 10.1007/s10853-008-2583-4

INTERFACE SCIENCE

# Field-assisted diffusion bonding and bond characterization of glass to aluminum

**C. R. Liu · J. F. Zhao · X. Y. Lu · Q. S. Meng · Y. P. Zhao · Z. A. Munir**

Received: 12 December 2007 / Accepted: 5 March 2008 / Published online: 31 March 2008
© Springer Science+Business Media, LLC 2008

**Abstract** The bonding of glass wafers to aluminum foils in multi-layer assemblies was investigated by the field-assisted diffusion bonding process. Bonding was effected at temperatures in the range 350–450 °C and with an applied voltage in the range 400–700 V under a pressure of 0.05 MPa. The experimental parameters of voltage and temperature were the main factors in influencing the ionic current leading to the formation of the depleted layer. The peak current in three-layer samples (glass/aluminum/glass) during bonding is twice that for the case of the two-layer samples (aluminum/glass). SEM and EDS analyses showed the presence of transition layers near the glass/aluminum interface, and XRD data demonstrated the phase structure of the glass/aluminum interface. The tensile strength of the bonded material increased markedly with increasing temperature and applied voltage. Fracture occurred in the glass phase near the interface with the aluminum. Finite element analysis showed the residual deformation in three-layer samples to be significantly lower than in two-layer samples. The symmetry in three-layer samples resulted in the absence of strain, an important advantage in MEMS fabrication.

C. R. Liu · X. Y. Lu · Q. S. Meng (✉)
Department of Materials Science & Engineering, Taiyuan University of Technology, Taiyuan 030024, China
e-mail: mengqingsen1950@yahoo.com.cn

J. F. Zhao · Z. A. Munir
Department of Chemical Engineering & Materials Science, University of California, Davis, CA 95616, USA

Y. P. Zhao
Mechanical Research Institute of the Chinese Academy of Science, Beijing 100086, China

## Introduction

Field-assisted diffusion bonding or anodic bonding is a key technique in the joining of alkali-rich glass (or ceramics) to semiconductors or metals. The technique, first described by Wallis and Pomerantz in 1969 [1], has become an important process in the formation and assembly of micro-electromechanical systems (MEMS), pressure sensors, accelerometers, and microfluidic devices [2–4].

Field-assisted diffusion bonding has been extensively investigated to join glass to silicon [5]. Investigations have also been carried out for bonding of glass to other materials, including $SiO_2$ [6], $Si_3N_4$ [7], and various metals [8–10]. Bonding is effected by imposing a DC field across the glass-silicon layers at typical temperatures in the range 350–400 °C, with the glass being biased as the cathode. The field causes the dissociation of the alkali oxides in the glass and results in the migration of the metal ions (typically $Na^+$) away from the interface creating a depletion layer. The subsequent diffusion of oxygen ions to the silicon and the ensuing reaction to form Si–O bonds contribute to the bonding process [11, 12]. The microstructure and the composition related to the formation of the bond have been investigated [13–15].

Requirements in more complicated circuitry and micro-electrical devices have led to a focus on multi-layers of glass-metal entities for such applications as silicon ink-jet printers, biomedical devices, and micro-chemical analyzing system [16–18]. In the previous investigations on field-assisted diffusion bonding of glass-metal systems [19–22], layers of silicon, aluminum, or silicon nitride were prepared by sputtering or physical vapor deposition techniques. In the present article, the bonding mechanism and the factors influencing bonding of glass to aluminum are investigated in multi-layer systems, utilizing aluminum foils and glass wafers.

## Experimental materials and methods

Glass wafers, Pyrex 7740 (obtained from Corning Corporation), were used in the present work. Their chemical composition is given as (wt%) 80.9 $SiO_2$, 12.7 $B_2O_3$, 2.3 $Al_2O_3$, and 4.0 $Na_2O$. The roughness of the glass wafers (Ra) is less than 0.1 μm and their thermal expansion coefficient is $2.8 \times 10^{-6}$ °C$^{-1}$. The aluminum foils (99.997% pure, obtained from Alfa Aesar, Ward Hill, MA) are 0.02 mm thick and have a thermal expansion coefficient of about $25.6 \times 10^{-6}$ °C$^{-1}$. The glass wafers and aluminum foils were cut into pieces with dimensions of $10 \times 10 \times 0.4$ mm and $10 \times 10 \times 0.02$ mm, respectively.

Before each experiment, the foils and wafers were cleaned ultrasonically in methanol and acetone, and then dried with hot air. A schematic of the apparatus used in this investigation is shown in Fig. 1. The three-layer sample of glass/aluminum/glass is positioned on the bonding platform inside the bonding oven in such a way that the aluminum film was electrically connected to the anode and the two glass wafers connected to the cathode. A low pressure of 0.05 MPa was exerted between the anode and the cathode. When the temperature in the oven reaches a targeted value, a voltage is applied and the resulting current was recorded by a digital load cell (Mettler Corporation). The bonding process was conducted under voltages in the range 400–700 V and at temperatures in the range 350–450 °C. The time of application was 15 min in all cases. At the end of each experiment, the sample was cooled to room temperature at a rate of 1 °C s$^{-1}$. The samples were then cleaned with HCl solution to remove the alkali salt on the surface of the glass.

The bonded samples were glued to aluminum rods by epoxy resin adhesive. The bonding strength was evaluated using an Instron machine (Instron 5544, USA). Other samples were mounted, sectioned perpendicular to the metal interfaces, and prepared metallographically. The microstructure of samples was evaluated using scanning

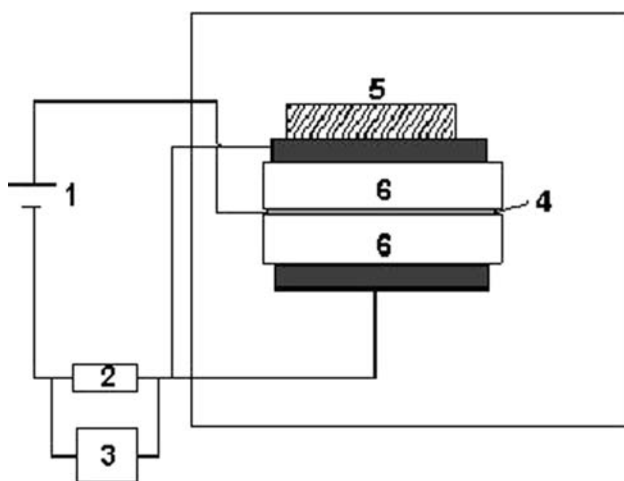


**Fig. 1** A schematic of the field-assisted diffusion bonding apparatus of three-layer glass/aluminum/glass sample. 1, D.C power supply; 2, resistance; 3, current recorder; 4, aluminum; 5, pressure controller; and 6, glass

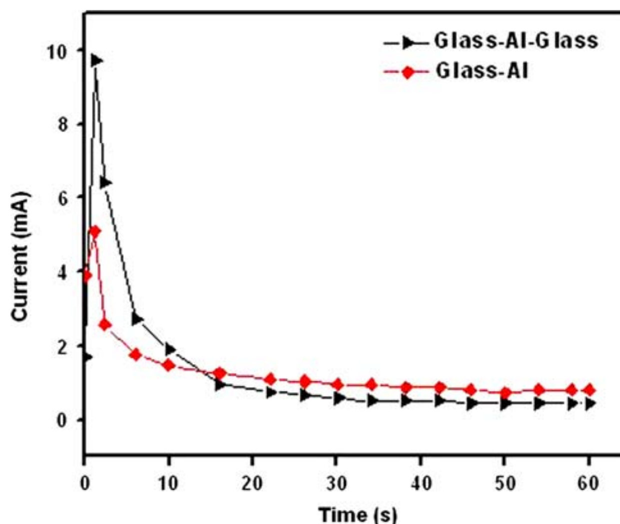


**Fig. 2** The bonding current of three-layer (glass/aluminum/glass) and two-layer (aluminum/glass) samples as a function of time at 450 °C with 600 V

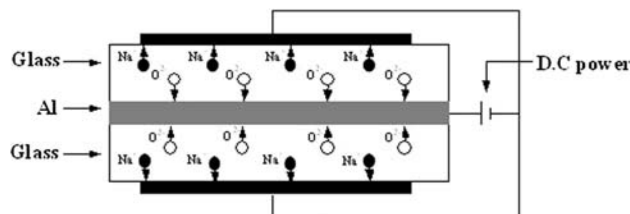


**Fig. 3** Mechanisms of the field-assisted diffusion bonding of glass/aluminum/glass

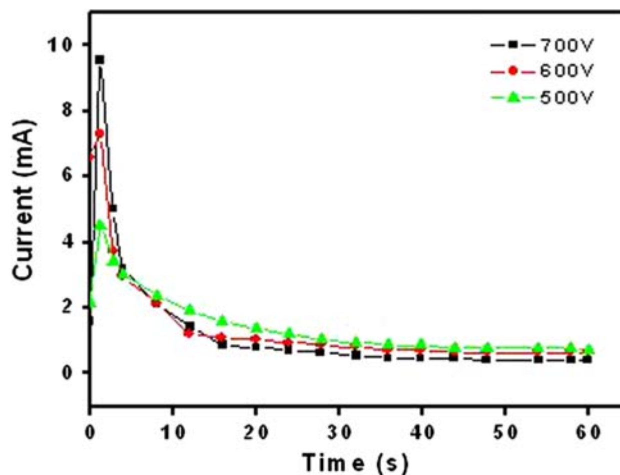


**Fig. 4** The current–time profiles during the field-assisted bonding of glass/aluminum/glass samples at various voltages at 450 °C

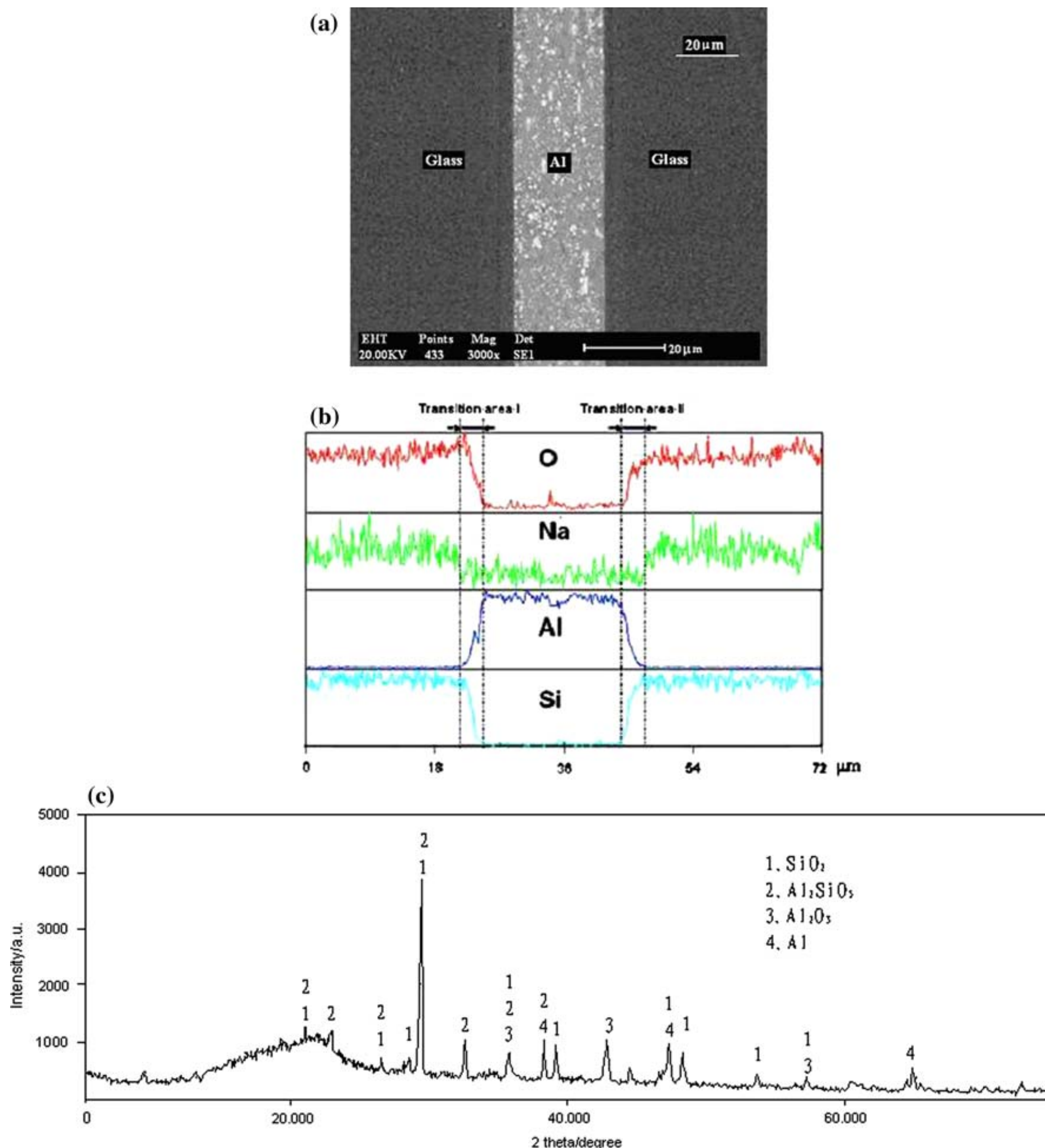


**Fig. 5** (**a**) Back-scattered electron image of three-layer bonded sample annealed with 600 V at 450 °C for 15 min; (**b**) EDS elemental concentration profiles of the sample in (**a**); (**c**) XRD patterns of glass/aluminum interface

electron microscopy (SEM). Distribution of the elements was determined by energy dispersive spectrometry (EDS). The phase structure of glass/aluminum interface was characterized by X-ray diffraction (XRD).

## Results and discussion

### Current–time characteristics

The external current was measured during field-assisted diffusion bonding and the results are shown in Fig. 2 for aluminum/glass and glass/aluminum/glass samples. The changes in the current with time represent two competing effects. Initially, the current increases rapidly as the area of intimate contact between the two materials being bonded increases. Simultaneously, the formation of the depletion layer due to the migration of the alkali cation causes a rapid decrease in the polarization current [23]. It can be seen in Fig. 2 that the peak current during the bonding of the three-layer sample (glass/aluminum/glass) was twice that of the two-layer sample (aluminum/glass) under the same conditions. Due to the effects of the electrostatic force and high temperature, sodium ions in the glass move toward the

cathode symmetrically at the two interfaces of the glass/aluminum as shown in Fig. 3. In the bonding process the $Na^+$ depletion layers on both sides of the aluminum foils were widened at the same time, and the strong electrostatic force was formed. This implies that the field-assisted diffusion bonding of the three-layer samples can be considered as two parts of glass/aluminum field-assisted diffusion bonding in parallel.

Figure 4 shows the effect of the applied voltage on the peak current at a constant temperature, 450 °C. As the voltage is increased from 500 to 700 V, the peak current increased markedly, from 4.6 to 10 mA. For bonding without the application of pressure and with a low pressure (~0.05 MPa), the contact between layers is affected by the electrostatic pressure resulting from the migration of the cations [23]. Since the latter process is dependent on the magnitude of the applied field, higher contact is expected with higher applied voltage, as seen in Fig. 4.

## Microstructure of the bond area

The micrograph shown in Fig. 5a is a back-scattered electron (BSE) SEM image of a three-layer (glass/aluminum/glass) sample bonded with 600 V at 450 °C for 15 min. The image shows the establishment of good contact between the glass and aluminum and the absence of porosity at the chosen magnification. There are no cracks, pores, or gaps at the two interfaces between the glass and aluminum. Figure 5b shows the concentration profiles of oxygen, sodium, aluminum, and silicon obtained from the EDS analyses. There are five distinct regions observable in these profiles: glass, transition area I, aluminum, transition area II, and glass. The concentrations of silicon, oxygen, aluminum, and sodium are symmetrically graded in both transition areas. The XRD patterns of the glass/aluminum interface demonstrated the transition layer mainly contains $Al_2SiO_5$ and $SiO_2$, as well as a small amount of $Al_2O_3$, as can be seen in Fig. 5c.

It is generally accepted that the formation of an oxide layer is the step that leads to the establishment of a good bond. In a recent investigation by Xing et al. [8] on bonding between glass and aluminum it was concluded that the diffusion of aluminum into the depletion layer within the glass is responsible for bond formation. In contrast, van Helvoort et al. [14] reported the formation of crystalline $\gamma$-$Al_2O_3$ when bonding was done at 450 °C. No crystalline oxide was detected when bonding was done at 350 °C. Referring to Fig. 5b, c, the present results show that aluminum has diffused into the depleted layer. While this analysis does show the diffusion of Al, it does not rule out the formation of an oxide. In the work of van Helvoort et al. [14] it was shown that both oxide formation and aluminum migration occur during the process of the bonding.

## Mechanical property characterization

Figure 6 and Table 1 show that the joining ratio increased from 69 to 88% and the tensile strength increased from 8.8 to 17.6 MPa as the bonding temperature increased from 350 to 450 °C. The joining ratio increased from 78 to 86% and the tensile strength was more than doubled (11.3–23.5 MPa) as the voltage increased from 400 to 700 V. The linear relationship between the tensile force and the tensile displacement, shown in Fig. 7, indicates that the cracking process is of a brittle rupture. The fracture occurring within the glass is due to the stress concentration in the brittle glass. The crack was initiated at the edge of the glass and propagated in the glass matrix.

## Analysis of interfacial residual stress

Analysis of the residual stress in the bonded samples was made by nonlinear finite element simulation with the

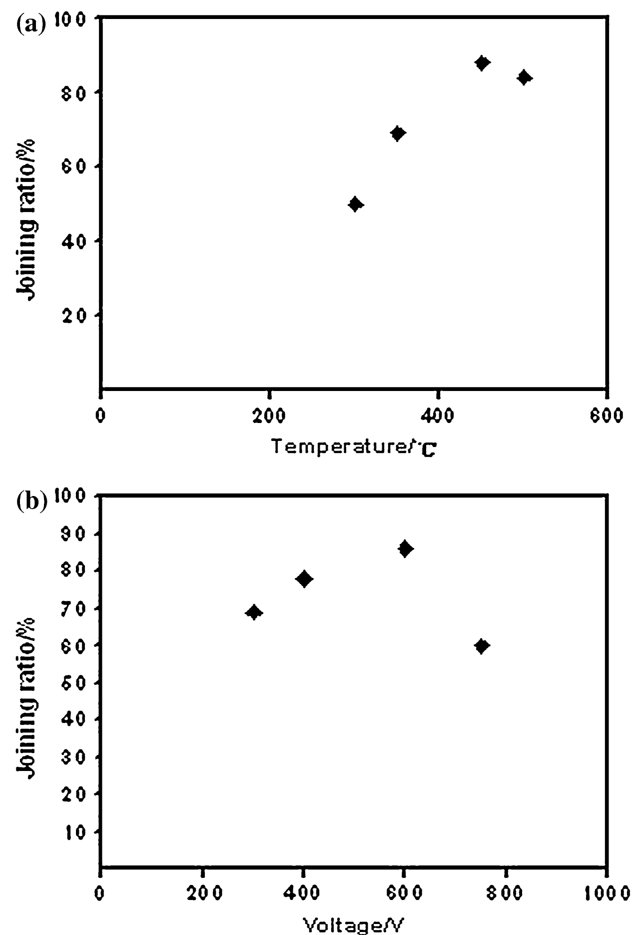


**Fig. 6** The effect of temperature and voltage on joining ratio of the glass/aluminum/glass field-assisted diffusion bonded samples. (**a**) Joining ratio versus bonding temperature and (**b**) joining ratio versus applied voltage

**Table 1** Tensile strength versus bonding temperature and applied voltage

| | Temperature (°C) | | | Voltage (V) | | |
|---|---|---|---|---|---|---|
| | 350 | 400 | 450 | 400 | 600 | 700 |
| Tensile strength (MPa) | 8.835 | 10.969 | 17.621 | 11.263 | 16.353 | 23.449 |

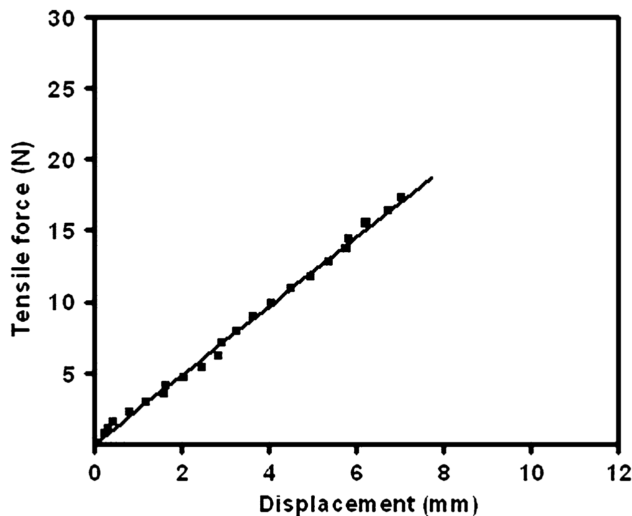


**Fig. 7** The relationship between the tensile forces and the displacements of glass/aluminum/glass bonded samples reacted with 500 V at 400 °C for 15 min

software MARC, and with aluminum as a plastic material. The results of two-layer (aluminum/glass) bonded samples were compared with those of three-layer (glass/aluminum/glass) samples. The dimensions of the samples used in this model are: aluminum foil, 2.0 × 2.0 × 0.02 mm; glass wafer, 2.0 × 2.0 × 0.4 mm. Because of the symmetry of the sample structure, the origin of coordinates was at the bottom center of the bonded sample. To simply compute, a quarter of each sample was analyzed. The transition layer was considered to be a film of $Al_2SiO_5$. The residual stress was calculated to represent samples cooled from 400 °C to room temperature.

The simulation results of two-layer bonded sample are shown in Fig. 8. Figure 8a shows the entire deformation of two-layer bonded sample. The bonded samples curved toward the aluminum layer, with 0.175% as the maximum deformation. Figure 8b shows the equivalent strain along the thickness of the sample (BB′). The maximum strain, $2.38 \times 10^{-2}$, occurred at the aluminum layer close to transition layer. With this condition, also, the figure shows that the minimum strain occurred at the glass, with a value of $1.87 \times 10^{-3}$. Figure 8c shows the distribution

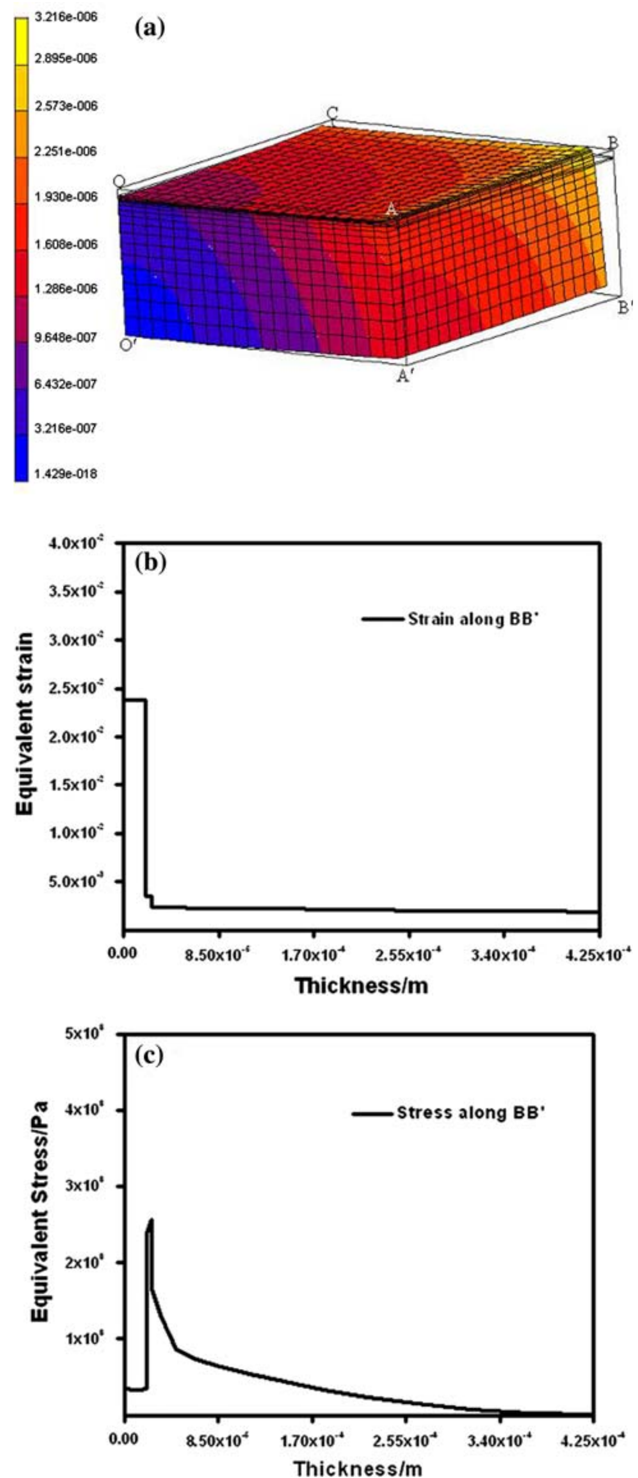


**Fig. 8** Finite element simulation of two-layer aluminum/glass bonded sample. (**a**) The entire deformation in two-layer aluminum/glass; (**b**) the equivalent strain of two-layer aluminum/glass; and (**c**) the equivalent stress of two-layer aluminum/glass

of the equivalent stress. The maximum stress occurs at the interface between aluminum and the transition layer, the value of which was 256 MPa.

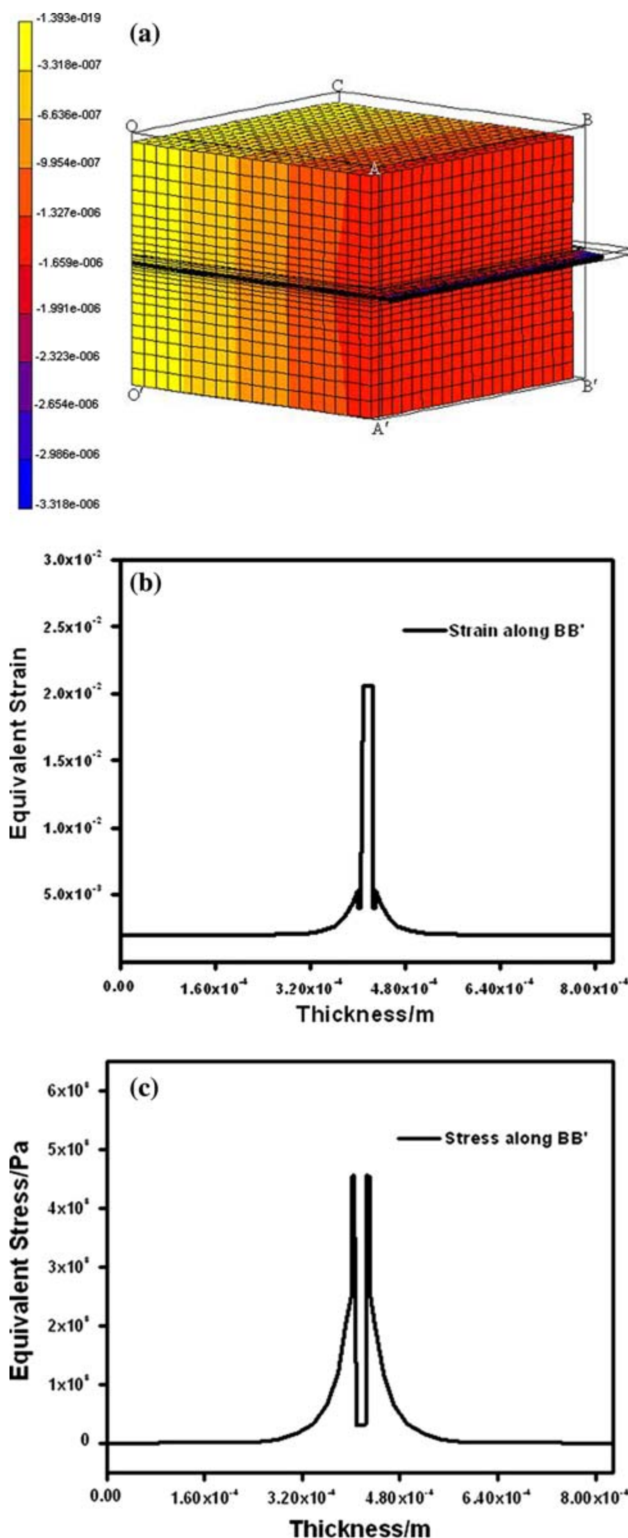


**Fig. 9** Finite element simulation of three-layer glass/aluminum/glass bonded sample. (**a**) The entire deformation in three-layer glass/aluminum/glass; (**b**) the equivalent strain of three-layer glass/aluminum/glass; and (**c**) the equivalent stress of three-layer glass/aluminum/glass

Corresponding to Fig. 8a, Fig. 9a depicts the deformation of the entire three-layer bonded sample, with 0.00418% as the maximum deformation. Figure 9b shows the equivalent strain along the thickness of the sample (BB′). The maximum strain, $2.06 \times 10^{-2}$, occurred at the aluminum layer. It can be seen that the deformation and equivalent strain in this sample is much smaller than that of the two-layer sample. Figure 9c shows that the equivalent stress along the edge of the sample, the equivalent stress of transition layer is much larger than that in other areas of the sample. Its maximum value is 456 Mpa.

The simulation indicated that due to the symmetry in the three-layer sample, the strain values at both sides of the aluminum layer offset each other, leading to the elimination of strain, a circumstance that is important in the sealing process of MEMS.

## Summary and conclusions

Three-layer samples of glass wafers and aluminum foils were successfully bonded by the field-assisted diffusion bonding process. Bonding was achieved at temperatures in the range 350–450 °C and with an applied voltage in the range 400–700 V. A low pressure of 0.05 MPa was applied during the process of bonding. The peak current during bonding of the three-layer (glass/aluminum/glass) samples is two times larger than that of the two-layer (aluminum/glass) samples at the same experimental conditions, indicating that the bonding of the former can be considered as two parts of the latter in parallel. The bonding process was mainly influenced by voltage and temperature. Mechanical characterization showed that failure represents a brittle rupture, which takes place in the glass matrix instead of the interface region. Modeling studies showed that the entire deformation and the equivalent strain in the three-layer samples are significantly smaller than those in the two-layer samples. The symmetry in the three-layer samples contributed to the absence of strain, an important advantage in MEMS fabrication.

**Acknowledgements** The present study was supported by grants (No. 50375105 and No. 50671070) from the National Nature Science Foundation of China. Professors Liu and Meng acknowledge the help of members of Professor Munir's research group during their sabbatical stay at his laboratory. We would also like to acknowledge the researchers of the Mechanical Research Institute of Chinese Academic of Science for their help with the modeling study. Support of this project to one of us (ZAM) by the US Army Research Office is gratefully acknowledged.

## References


1. Wallis G, Pomerantz DI (1969) J Appl Phys 40:3946. doi:10.1063/1.1657121
2. Shoji S, Kikuchi H, Torigoe H (1998) Sens Actuators A 64:95
3. Makino E, Mitsuyama T, Shibata T (2000) ibid A 79:251
4. Sasaki G, Fukunaga H, Suga T et al (1997) Mater Chem Phys 51:174
5. Rogers T, Kowal J (1995) Sens Actuators A 46–47:113. doi:10.1016/0924-4247(94)00872-F
6. Plaza JA, Esteve J, Lora-Tamayo E (1998) Sens Actuators A 67:181. doi:10.1016/S0924-4247(97)01739-1
7. Weichel S, deReuss R, Bouaidat S et al (2000) Sens Actuators A 82:249. doi:10.1016/S0924-4247(99)00372-6
8. Xing QF, Sasaki G, Fukunaga H (2002) J Mater Sci Mater Electron 13:83
9. Morsy MA, Ishizaki K, Ikeuchi K et al (1998) Quart J Jpn Weld Soc 16:157
10. Briand D, Weber P, de Rooij NF (2004) Sens Actuators A 114:543. doi:10.1016/j.sna.2003.10.070
11. Wallis G (1970) J Am Ceram Soc 53:563
12. Albaugh KB, Rasmussen DH (1992) ibid 75:2644
13. Gossink RG (1978) J Am Ceram Soc 61:539
14. van Helvoort ATJ, Knowles KM, Fernie JA (2003) J Am Ceram Soc 86:1773
15. Borom MP (1973) J Am Ceram Soc 56:254. doi:10.1111/j.1151-2916.1973.tb12482.x
16. Beatty CC (1996) Technical digest solid-state sensor and actuator wordshop. Transducer Research Foundation 200:204
17. Sobek D, Senturia SD, Gray ML (1994) Technical digest solid-state sensor and actuator wordshop. Transducer Research Foundation 260:263
18. Harrison DJ, Fluri K, Chiem N (1996) Sens Actuators B 105:109
19. Despont M, Gross H, Arrouy F (1996) Sens Actuators A 55:219. doi:10.1016/S0924-4247(97)80081-7
20. Nimkar ND, Bhavnani SH, Ellis CD (2004) Sens Actuators A 113:212. doi:10.1016/j.sna.2004.02.028
21. Huff MA, Schmidt MA (1992) Technical digest IEEE solid-state sensor and actuator workshop. IEEE 194:197
22. Epstein AH, Senturia SD, Anathasuresh G (1997) Technical digest IEEE solid-state sensor and actuator wordshop. IEEE 753:756
23. Knowles KM, van Helvoort ATJ (2006) Int Mater Rev 51:273